The characterisation of arsenic plasma doping and post implant processing of silicon using medium energy ion scattering

Running title: As Plasma doping of Si analyzed by MEIS

Running Authors: Van den Berg et al.

Jaap van den Berg[a)] and Andrew Rossall

Ion Beam Centre, School of CSE, University of Huddersfield, Huddersfield, HD1 3DH, UK

Jon England

Varian Semiconductor Business Unit, Applied Materials Inc.,35 Dory Road, Gloucester, MA 01930, USA

[a)] Electronic mail: j.vandenberg@hud.ac.uk

Plasma doping (PLAD) is increasingly applied in micro-electronic device manufacture to produce high throughput, high fluence implants. In this medium energy ion scattering (MEIS) study of the PLAD process, Si(100) wafers were exposed to a As containing plasma while pulse biased negatively to 7 kV to cause (recoil) implantation and deposition of As. Quantitative MEIS depth profiling analysis in conjunction with energy spectrum simulation was applied to characterize the near surface layer changes of the Si wafer following i) the PLAD process, ii) two types of chemical wet clean (oxidizing and non-oxidizing) and iii) spike annealing in a N_2 atmosphere.

MEIS analysis showed that the PLAD process produced an intermixed As/Si layer, with a near-surface As content of ~ 40% that decayed almost linearly to near-zero at a depth of ~17 nm. This mixed As/Si layer was unstable in air and the initially recorded 1.2 nm

thick oxide cap layer grew over a period of 4 months to 3.5 nm with a concurrent 25% As loss by sublimation.

The application of the industry standard, oxidizing wet chemical clean removed the top As and concurrently produced a ~14 nm thick Si oxide above the remaining implanted As profile, which matched the tail of original As implant profile. As depth profiles measured for the 7 kV PLAD process after a wet clean and spike annealing showed solid phase epitaxial regrowth (SPER) of the disordered layer. A detailed comparison of the random and aligned MEIS spectra yielded depth profiles of substitutional As with a concentration in excess of 1 $x10^{21}$ As cm^{-3} over a depth greater than 10 nm. The retained dose of 1.35 $x10^{15}$ cm^{-2} represents a ~70% increase in substitutional As compared to that recorded after a non-oxidizing clean.

Such an alternative wet chemical clean, in which Si re-oxidation did not occur, was applied to determine the depth of the mixed As /Si layer removed. Found to be 7 nm, the analysis indicated that the etching process ceased when the Si concentration reached 4 $x10^{22}$ cm^{-3}. After spike annealing part of the remaining As had segregated in a thin layer under a 1.6 nm thick surface oxide. The retained As dose in this case was 8 $x10^{14}$ cm^{-2}, equivalent to a 1% As substitutional dopant concentration to a depth of ~14 nm.

Different substitutional As doses measured with MEIS were found to correlate closely with sheet resistance measurements, confirming that equating the substitutional As with the active As dose remains correct for these ultra-shallow profiles, typically 10 nm deep.

I. INTRODUCTION

Plasma doping (PLAD) has become an important process for implanting micro-electronic devices since it enables high fluence ion implantation of low energy dopants with high throughput for e.g. DRAM (dynamic random-access memory) polysilicon gate doping as well as conformal doping applications[1,2]. These processes have been widely adopted by leading device manufacturers across multiple transistor technologies. During PLAD, a silicon wafer is processed inside a chamber where it is immersed in an inductively coupled plasma that contains the ion species to be implanted and the wafer is pulse biased negatively to between 0.1 and 12.0 kV [3]. The bias potential causes the formation of a plasma sheath above the wafer across which plasma ions are accelerated and implanted into the Si wafer surface. In addition to ion implantation, deposition of neutral species occurs as do recoil implantation of deposited atoms and sputtering and, depending on the species present in the plasma, reactive ion etching. These multiple processes make PLAD a multifaceted overall process to model. Although efforts have been undertaken to incorporate understanding of these mechanisms to improve process modelling [4] they are hampered by the comparative dearth of reliable experimental data on the dependence of the shape of implant profiles, as implanted, retained and indeed active doses on the overall PLAD process parameters and subsequent processing.

The lack of such metrology information is in no small measure due to the difficulty that sputter depth profiling techniques such as secondary ion mass spectrometry (SIMS) have in providing quantitative profiling information on the PLAD produced, ultra-shallow (say, 0-15 nm deep) region that is not distorted by effects such as transient sputter rates, collisional mixing and, especially for SIMS, matrix effects. Despite these

limitations, SIMS depth profiling has been shown, in specific circumstances, to be capable of a quantitative determination of dopants profiles located across and below oxide layers by combining the technique with another, such as angle resolved XPS (ARXPS) to determine PLAD produced B profiles[5], or by a careful calibration of SIMS data of shallow beamline As implants against medium energy ion scattering (MEIS) results to provide appropriate corrections factors for the measured depth profile[6]. Using this protocol, As depth profiles produced by non-pulsed, high dose plasma immersion ion implantation (PIIID) were quantified within the post PIIID grown surface oxide and going across it into the mixed As/Si layer. This enabled As dose retained in the As rich regrown oxide as well as its loss over time, to be determined[7,8]. This work also identified the formation of arsenolite microcrystals on the wafer surface.

Unlike SIMS depth profiling, ion backscattering techniques do not suffer from the limitations mentioned above. However, their detection sensitivity is much inferior to that of SIMS. Rutherford Backscattering (RBS) using a surface barrier detector is quantitative[9] but does not possess the depth resolution required to resolve PLAD produced shallow implants. Medium energy ion scattering (MEIS) analysis[10,11] on the other hand, through the use of a high resolution electrostatic energy analyser, is capable of providing quantitative dopant and disorder depth profiles down to ~nm resolution as demonstrated for ultra-shallow beamline implants[6,12,13]. XTEM linked energy dispersive X-ray spectroscopy (EDS) is another analytical technique capable of elemental mapping, yielding depth profiles which have a comparable resolution to MEIS. It can also provide lattice and disorder imaging, but unlike MEIS the method requires individual sample preparation and provides only atomic fractions rather than atomic concentrations.

In this study, MEIS has been applied to obtain a detailed characterisation of As depth profiles after 7 kV PLAD processing as well as of the changes to these distributions following wafer processing such as a wet clean and annealing. Importantly, through the recording and comparing of aligned and random MEIS energy spectra following spike annealing, substitutional dopant profiles and retained active fluences were determined. The information obtained forms a necessary starting point towards a better understanding of the complex processes occurring during PLAD as it provides the prerequisite accurate reference data for any dynamic modelling approach that is being pursued[4] to unravel the effects of the interacting processes of deposition, (recoil) implantation and sputtering during PLAD.

II. EXPERIMENTAL

Samples for MEIS analysis were cut from 12" Si (001) wafers that had undergone As PLAD implantation in a VIISta system at VSE, Applied Materials in Gloucester, MA, USA. The plasma was generated in a process chamber containing a low pressure AsH_3 gas mixture through an inductively coupled RF excitation [3]. To effect implantation, the wafer was biased negatively by a 7 kV pulse. The non-mass analysed ion implant dose as measured with a Faraday cup was $1x10^{16}$ cm^{-2}.

Arsenic depth profiles were derived from the MEIS spectra recorded i) post As PLAD treatment, ii) after applying an industry standard sulphuric peroxide mixture (SPM) chemical clean (a 70% sulphuric acid, 5.6% hydrogen peroxide and 24.4% water mixture) and iii) following thermal processing using a 5s 1000°C spike anneal in a N_2 atmosphere. Further to ii) MEIS spectra were also taken after an alternative wet clean (type 2 clean) in which Si oxidation did not take place and this enabled the thickness of

the layer removed by the etch to be determined. For reference, an overview of the various samples sequentially investigated by MEIS in this study with sample codes and their process conditions is given in Table I.

TABLE I. Sequence and process details of the samples analyzed.

Sample	Process conditions
AM1	7 kV As PLAD
AM3.1	7 kV As PLAD, SPM wet clean
AM3.2	7 kV As PLAD, SPM wet clean & spike anneal
AM2	7 kV As PLAD, non oxydizing clean
AM4	7 kV As PLAD, non oxydizing clean, spike anneal
AM3.9	7 kV As PLAD, SPM wet clean & spike anneal
AM3.10	7 kV As PLAD, SPM wet clean & spike anneal

Analysis of these samples was performed at the MEIS facility at the University of Huddersfield (UK) under UHV (low 10^{-9} mbar) conditions using 100 keV He^+ ions scattered through 90º in a double alignment configuration with the beam incident along the [-1-11] direction (54.7º off normal) and the analyser aligned with the [112] direction. The resulting scattering angle of 90º represents an optimum compromise between separation of the Si and As peaks and hence the maximum As depth that can be recorded, depth resolution, backscattering yield and available double alignment conditions. For annealed samples, spectra were also taken under random incident and exit directions achieved by changing the angle of incidence to 61.7° and spin angle by 7° of the sample whilst maintaining a 90º scattering angle in order to facilitate the determination of the As dose in substitutional Si lattice positions. Samples were analysed on receipt and selected

samples (e.g. AM1) reanalysed after a period of time in order to monitor any release of As from the surface.

MEIS energy spectra were converted into depth profiles in two different ways. In the first method, concentration depth profiles of As were obtained by direct conversion of the MEIS energy spectra, using the surface approximation[14] and inelastic energy loss rates obtained from SRIM [13,15] while referencing the As scattering yield to the random Si yield at the surface edge and equating this to the Si density, whilst making appropriate corrections detailed below. Using the second method, MEIS spectra were fitted using a spectrum simulation program, from which the "best fit" depth profiles for the bulk constituents were derived. Brief details of the simulation model which operates within the IGOR6 PRO© graphing software[16] are given in ref. [17]. In both cases the Si bulk density was used in the calculations. Strictly, in ion scattering depth profiling, the depth scale is measured in terms of areal densities (atoms/cm^2). To enable comparison with other analytical techniques such as EDS or compare with process specifications, a depth scale in nm units is necessary. This requires knowledge or a reliable estimate of the density of a layer, which could be either the bulk density or a slightly smaller value. The use of a reduced value would lead to an inversely proportional increase of the depth scale in terms of nm. Such a choice may then be justified through comparison with another direct technique or on the basis of other information, as e.g. done in Section B1.

Both approaches include the screening correction using the Andersen formalism[18] as well as an energy dependent neutralisation correction based on the best available data in order to improve the quantification of the results obtained[17]. Compared to spectrum simulation using the IGOR based model, the direct spectrum conversion has the

advantage of providing the atomic concentration vs. depth of the As implant, although shallow O profiles can rarely be extracted reliably due to the fact that the often small O signal is superimposed on a much larger background of disordered Si. On the other hand, whereas IGOR model simulations provide only atomic fraction vs. depth information of all species, they enable details of the oxide layer, e.g. its thickness to be determined.

III. RESULTS AND DISCUSSION

A. PLAD processed Si

The first set of samples analysed with MEIS was cut from a wafer that was PLAD implanted to a nominal dose of $1x10^{16}$ cm^{-2} employing a 7 kV pulsed bias voltage. One sample was inserted upon receipt into the MEIS analysis chamber operating at ultrahigh vacuum (uhv) and then reanalysed after being left in air for 17 days and 4 months, respectively. They are referenced as post PLAD sample AM1 (uhv), AM1 (17 days) and AM1 (4 months), respectively. The objective was to determine the post implant As, Si and O profiles and monitor any profile evolution after exposure to air. MEIS spectra for these samples taken after the different time lapses are shown in Figure 1 by the data points. In all three cases the energy spectra show peaks due to scattering off As (marked As) each having a near-triangular shape, as well as rounded off Si edges, which for a clean Si sample, would normally be sharp as approximately indicated by the dotted lines, and finally, a small peak due to scattering off O. The spectra show that upon exposure to air for longer periods i) the As peak reduces in area, ii) its high energy edge moves to a lower energy and iii) the oxygen peak (O) grows in size. These observations indicate the loss of As and growth of a surface oxide, as also observed in [7,8]. These changes coupled

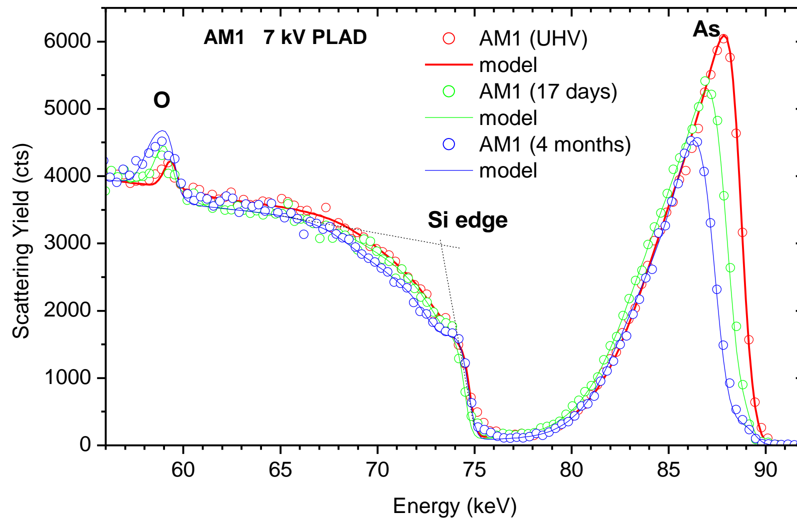

FIG. 1. MEIS energy spectra of the PLAD treated sample AM1 showing a mixed As/Si layer taken at 3 stages of exposure to the air: on receipt (uhv), after 17 days and after 4 months, at which stage it shows a 25 % As loss.

with the observation that the MEIS energy spectrum for a sample left in uhv for 17 days (not shown in Figure 1) did not show any change compared to the as-received implanted sample AM1(uhv), confirm that oxidation is the cause for the changes in the energy spectrum and the driver for the observed As loss.

MEIS spectra for as-implanted samples shown in Figure 1 were modelled using the IGOR based simulation code and the best fit spectra (model) have been added to the figure. Depth profiles of the Si, As and O atoms in terms of atomic fractions, derived from the best fit for the as received implanted sample AM1 (uhv) are shown in Figure 2 by the solid lines to a depth of 20 nm. Reflecting the shape of the As peak in the MEIS

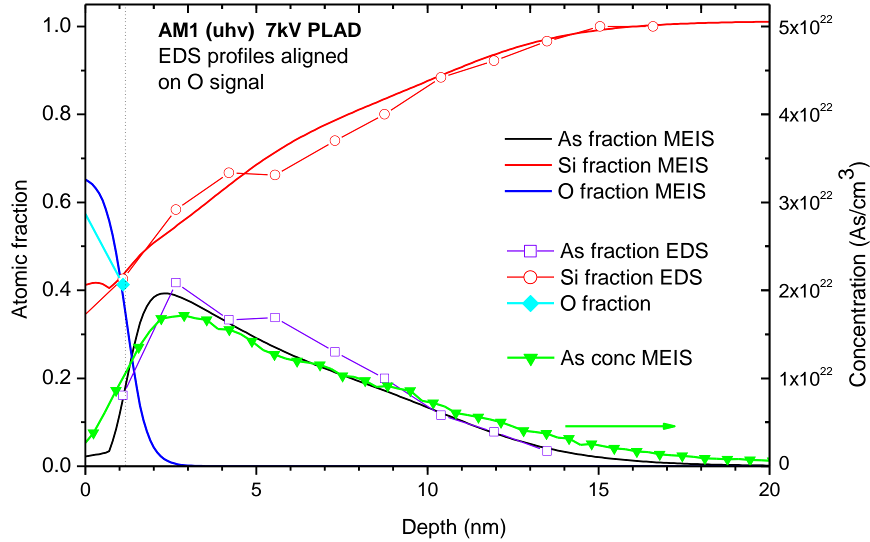

FIG. 2. Simulated best fit, fractional depth profiles of As, Si and O of sample AM1 (uhv), compared with directly converted As concentration depth distributions (RH scale) and with fractional EDS determined depth profiles. Lines are drawn to guide the eye.

energy spectrum, the As depth profile for this sample similarly has a triangular shape with a ~40 % near-surface As fraction. Implanted As replaces silicon in the matrix and the resulting Si matrix dilution is reflected in the Si profile, which is almost a mirror image of the As depth profile. Figure 2 shows that As is located underneath a thin Si oxide layer of 1.2 nm thickness, indicated by the dotted vertical marker. It should be mentioned that a fit could only be achieved by assuming that the oxide contains no As. Simulations for the other two as-implanted samples also shown in Figure 1 indicate a growth of the oxide layer to 1.9 nm after 17 days, and to 3.5 nm for this sample after 4 months, about half the rate observed in Ref. [8]. This growth results in a shift of the high energy As edge to lower energies due to the energy loss of the particle beam in the top oxide as is seen in Figure 1 and corresponding shifts of the As profiles to a greater depth. The growth of the oxide is also reflected in the formation of a narrow ledge in the Si

profile at around 74 keV due the reduced Si fraction within the silicon oxide. These clearly observable shifts demonstrate the nanometre scale sensitivity of MEIS to the thickness of the oxide layer through which the ions are passing on their way in and out.

Also presented in Figure 2 al is the As depth distribution obtained by a direct conversion of the MEIS energy scale of the As peak into a depth scale using the surface approximation and the SRIM derived inelastic energy loss rates whilst equating the ion yield at the Si edge to the Si density. This comparison was performed to i) check the reliability of the As depth scale obtained from the IGOR model simulation and ii) to compare the atomic fractional data of the simulation (LH scale) with the concentration data obtained from the direct conversion (RH scale). For ii) the two vertical scales need to be equated at the points of 100% Si and Si density of 5 x 10^{22} cm^{-3}. Figure 2 shows that the profiles shapes are well matched with the peak As concentration of 2 x 10^{22} cm^{-3} corresponding to a ~40% As fraction, as simulated. The slightly shorter range calculated in the simulation is caused by i) the greater stopping due to the incorporation of the As into the Si matrix in the IGOR model ii) the deconvolution of the MEIS broadening, not accounted for in the direct conversion but, as Figure 2 shows, the difference is not significant.

As a check on the overall depth scale, the MEIS derived profiles for As and Si in Figure 2 were next compared with those obtained from EDS analysis during XTEM investigation of these samples[19]. These EDS depth profiles of the atomic fractions of As and Si and O have been added to Figure 2, based on the criterion that the oxide interface should align for both MEIS and EDS (at 1.2 nm depth on the MEIS depth scale). The correspondence of the two depth scales and the atomic fractions of the profiles obtained

by the two methods is good and the overall agreement between the different methods lends justification to the assumed Si bulk density for this mixed layer. It also gives confidence that not only the depth scales but also the relationship between atomic fraction obtained from the IGOR based code and concentration are reliable.

MEIS spectra in Figure 1 showed that near-surface part of the implanted As profile was unstable at the air, in that it shows an As dose loss over time which can be quantified. The area under the As peak of the as-implanted sample AM1 (uhv) equates to a dose of 1.6 x 10^{16} As cm^{-2} retained in the Si sample. After 4 months however the As dose loss is ~25% or, on average approximately 4 x 10^{13} As atoms per day, although the initial dose loss rate is likely to have been much higher.

B. PLAD, SPM wet clean and spike anneal

1. Post PLAD spectra

In this section, samples which in addition to PLAD at 7 kV had undergone i) an industry standard SPM clean (AM 3.1) and ii) a subsequent spike anneal (AM3.2) are analysed. Figure 3 depicts the aligned MEIS spectra for these samples. Aspects of the spectra to be noted are the presence of the substantial peak between ~55 and 60 keV due to scattering off oxygen, the reduced height of the Si peak between ~72 and 76 keV below the Si edge and the shift of the high energy edge of As peak to an energy lower by ~ 5 keV compared to that in Figure 1, where it appears at ~ 90 keV. They all result from the formation of a thick oxide layer on both samples. The lower Si yield at and below the

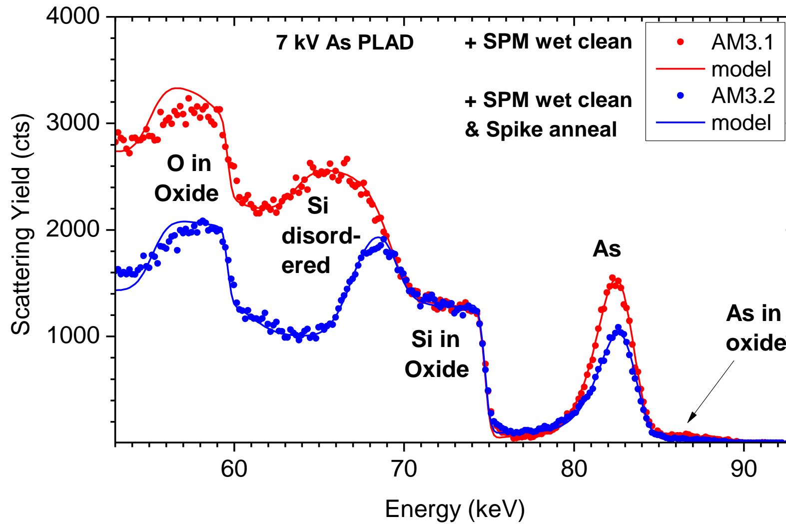

Figure 3. MEIS spectra and model simulations for sample AM3.1 (PLAD processed at 7 kV bias and SPM clean) and sample AM3.2 (with additional spike anneal).

Si edge for both samples is due to the reduced Si concentration in the oxide (nominally 44%) which is measured at 42±2% of the standard Si yield at the Si edge, recorded for a fully amorphised Si sample (spectrum not shown). Since the As profiles are located underneath this thick oxide, their lower energy is caused by the extra energy loss the He ions suffer when passing through the oxide. A further feature of the spectrum, in particular for sample AM3.1, is a broad disordered, higher yield Si region as marked in the figure, which is associated with the As implanted region.

The changes in the spectra going from post PLAD sample AM1shown in Figure 1 to post clean sample AM3.1 in Figure 3, reflect the changes produced in the wafer surface region due to the action of the SPM wet clean. Starting from the near-triangular As peak in Figure 1 representing the pre-wet clean state for sample AM3.1, it is seen that the SPM clean is effective in removing much of the As from the mixed As/Si layer as

demonstrated by the strongly reduced As peak height and width while, as the As is etched away, the peroxide concurrently converts the Si of the previously mixed layer into a SiO_2 layer which is measured to be 14.0 nm thick, as shown below.

A further observation in the spectrum for the post wet clean sample AM3.1 is the presence of a low-level scattering yield between 85 to 89 keV. This is due to scattering off residual As located within the oxide layer and indicates that the SPM wet clean is not totally effective in removing all of the As from the etched part of the mixed As/Si top layer. Depth profiles shown in Section B2 below show that As is present in the oxide at a concentration of ~$1x10^{20}$ cm^{-3}. Considering that during a SPER process As normally segregates out from the regrowing, ordered Si bulk into a very shallow layer that becomes trapped under the oxide into which it is not normally accommodated [12], this is at first sight surprising. On the other hand, it needs to be remembered that a thermal bulk diffusion process is rather different from a wet etch process, in which the oxide apparently can accommodate a low level of As. This may in fact reflect the formation of a low level of arsenolite (As_2O_3) observed in ref. [7,8], although the formation process in that case was oxidation in the air. It is also conceivable that a fraction of the As peak at 82 keV is due to a degree of “snow-plowing” of some As in front of the growing oxide during the etch/oxidation process during the SPM clean.

Next, the changes that occur in the MEIS spectrum going from post SPM wet clean (AM3.1) to post spike anneal (AM3.2) in Figure 3 are considered. Best fit model simulations are added for both samples. They illustrate the solid phase epitaxial regrowth (SPER) process whereby the post-clean disordered Si peak for sample AM3.1 is reduced to the much narrower surface Si peak after anneal for AM3.2. Depth profiles of the Si, As

and O species derived from the best fit simulations are depicted in Figure 4, which shows the formation of a stoichiometric SiO_2 layer which is 14 nm thick, assuming a SiO_2 density of 2.0 g cm^{-3}. This value, which is reduced by ~10% from the bulk figure was determined from Coulomb explosion experiments on a similar sample performed at the Federal University of Rio Grande del Sul (Br) [20]. The oxide thickness is again confirmed by XTEM measurements which yielded a marginally greater value of 14.3 nm[19]. Figure 4 clearly shows the SPER process that has reduced the width of the disordered region by

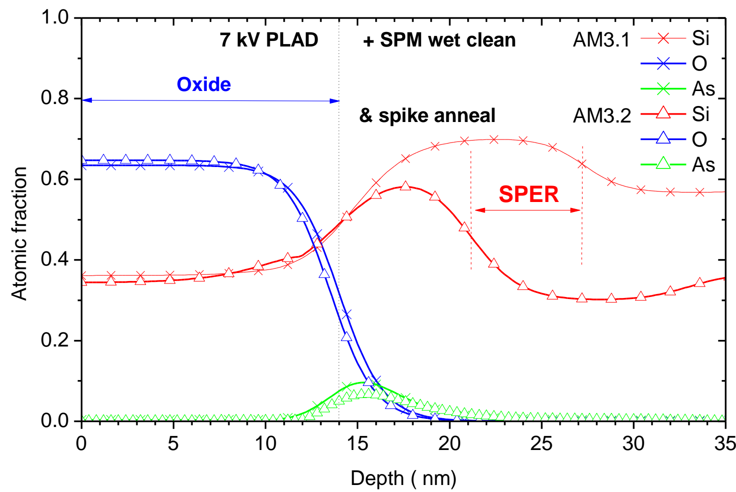

Figure 4. Best fit fractional depth profiles of As, Si and O of samples AM3.1 and AM3.2 showing the formation of a ~14 nm thick oxide in the SPM wet clean process and the epitaxial regrowth (SPER) following annealing.

~ 6 nm as marked, which closely matches the thickness of the disordered Si layer of 5 nm observed in the XTEM image[19]. A final observation in Figure 4 is the small reduction in the width of the oxide after the spike anneal which, if significant, may suggest minor oxide loss upon annealing.

2. *Post anneal Random and Aligned spectra*

Ion scattering performed in a random direction detects in principle all implanted dopant atoms in Si that are within the penetration range of the He ions and are heavier that the matrix species. However, in an aligned direction only those dopant atoms not in substitutional positions are visible to the beam[21]. Hence, careful comparison of MEIS spectra in double aligned and random directions enables the determination of the substitutional, or active dose in the shallow surface region. Note that the correlation between this substitutional dose and the sheet resistance will be considered in section F, where it is found that for this very near-surface doped layer, the usual identification between substitutional and active dose remains justified.

Whereas in RBS, because of the comparatively small critical angles resulting from the use of MeV light ions, it is comparatively straightforward to obtain a “random” direction for samples with a crystalline bulk, this is not generally the case for 100 keV He ions in MEIS which has much larger critical angles. In a detailed investigation the backscattering yield off a pre-amorphized Si sample was compared with that of sample AM4, (annealed after a type 2 clean and discussed in Section E below) for a number of different angles of incidence and azimuths. From this the angular conditions that gave an equivalent “random” Si background yields in Si were established and these were used for the random spectra presented in this and the following sections. If, as is the case in this section, the toplayer is SiO_2, then the Si yield reduces to 44% of that of bulk Si. In each case it is the ion yield at the SiO_2 or Si surface edge which is used for the determination of the As dose.

MEIS spectra were recorded for the aligned and random directions of incidence of sample AM3.2 (implanted, SPM cleaned and spike annealed at 1000ºC). Presented in Figure 5 they show the clear difference between the As peaks in the aligned and random spectra. Note that the Si signal originating from the Si oxide in the random spectrum is higher than that of the aligned spectrum due to its superposition onto the higher As background signal, caused by the As yield now appearing at lower energies.

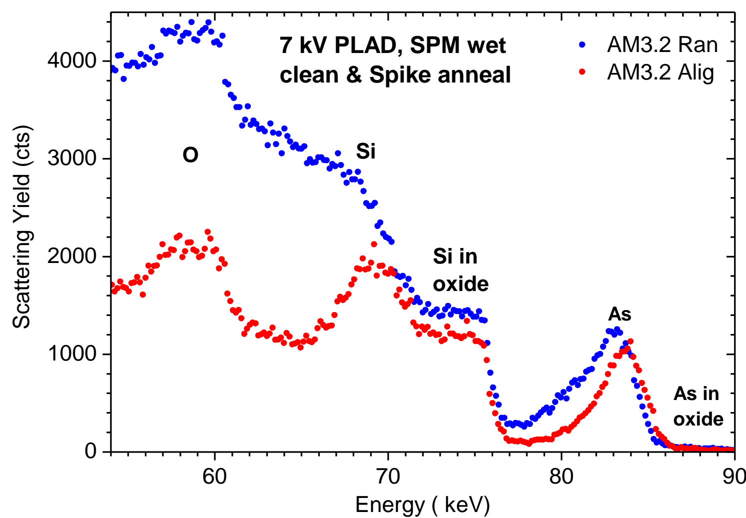

FIG. 5. MEIS energy spectra of sample AM3.2 (after 7kV PLAD, SPM wet clean and spike anneal) in random and double aligned configurations.

Concentration depth profiles obtained by direct conversion of the As peaks in the energy spectra of Figure 5 are shown in Figure 11 to a depth of 28 nm, beyond which peak interference due to the Si peak (in SiO_2) occurs. The conversion took into account the change in illumination of the of the target by the ion beam for the different angular conditions[22]. The As profile for the aligned sample obtained from the simulation has been added to the figure in which the RH scale gives the As atomic fraction. The agreement

between the two As profiles is good, taking into account that the simulation deconvolves the system broadening, which leads to a slightly narrower profile. Because the vertical scale in Figure 6 is only ~10% of the full range the simulated O depth profile is not shown but its half height is given by the dotted line as a mark of the depth of the oxide.

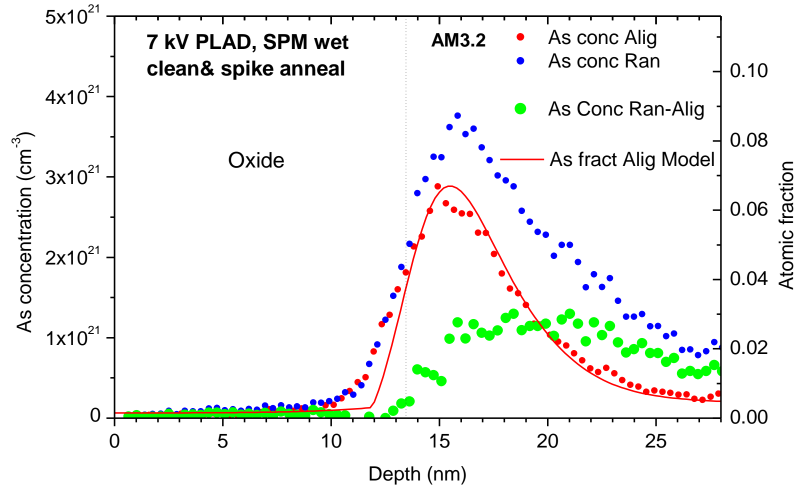

FIG. 6. As concentration depth profiles in sample AM3.2, taken in the random and aligned directions including the difference profile representing the substitutional As depth profile.

It is seen from Figure 6 that there are broadly two contributions to the As profile, i) a segregated (inactive) but now broader As peak between ~14 and 18 nm resulting from the spike anneal process and possibly the oxidation process moving As into the bulk of the sample and ii) a distribution of partly substitutional As largely beyond the depth of the segregated As. In view of the mentioned Si peak interference which starts to occur, the As doses for the two profiles and their difference are integrated between depths of 9 to 28 nm with the results presented in Table II. The substitutional As dose determined by MEIS analysis is found to be 1.35 x 10^{-15} cm^{-2} As.

TABLE II. Retained As doses after PLAD at 7 kV bias, SPM wet clean and spike anneal, as measured in the random and aligned directions. The substitutional As dose is given by their difference.

Sample	Integration over depth (nm)	As dose (cm^{-2}) Random	As dose (cm^{-2}) Aligned	As dose (cm^{-2}) Rand - Align (Subst. As)
AM3.2	9-28	3.4×10^{15}	2.05×10^{15}	1.35×10^{15}

C. PLAD, (non-oxidizing) wet clean and spike anneal

1. Post PLAD spectra

MEIS spectra for samples that have been treated with this type 2, non-oxydizing clean are considered in this section. The aim was to monitor the changes in the derived depth profiles after this type of wet clean in comparison with the PLAD processed sample AM1 (uhv) discussed in Section A. As will be shown, this particular clean has the effect of etching away the highly As doped Si region, rather than converting it into a thick Si oxide layer which occurred when the industry standard SPM clean was applied as shown in Section B. Thus, the thickness of the layer removed by the wet clean can be determined by MEIS. The depth profiles derived are next compared with those obtained with the full SPM clean applied, discussed in Section B. From a MEIS analysis point of view the absence of such a thick oxide layer has the advantage of providing better resolved MEIS spectra depth profiles, due to reduced straggling[14].

Double aligned MEIS spectra and corresponding model simulations following this type 2 wet clean sample AM2 and post-anneal sample AM4 are presented in Figure 7. Comparing these with those for the PLAD treated sample AM1 (uhv) (shown in Figure 1) added to this figure, the effects of the two processing stages are clearly visible. The main observation is a substantial reduction in height and width of the As peak for the post

clean sample AM2, confirming that the wet clean process has resulted in the removal of much of the As. The retained As dose, as measured by MEIS is reduced from 16 to 3 x 10^{15} cm^{-2}, i.e. to less than 20 % of the as-implanted As dose.

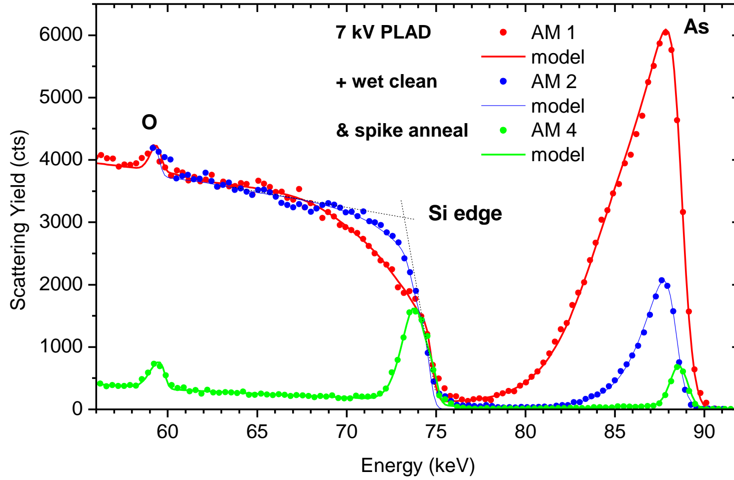

FIG. 7. MEIS energy spectra of the i) PLAD implanted sample AM1 (uhv), ii) post-wet clean sample AM2, and iii) post-spike anneal sample AM4.

The removal of most of the top mixed As/Si layer restores much of the sharpness of the Si edge in the energy spectrum of sample AM2, which is due to a more abrupt Si-vacuum interface following the wet clean process. Subsequent spike annealing shows the restoration of the crystallinity of the sample through solid phase epitaxial regrowth (SPER), evidenced by the removal of the disordered Si background below ~73.5 keV and the reduction of the As dose visible to the beam in the double aligned conditions employed, to ~ 4 x 10^{14} cm-^{2}.

The As, Si and O depth profiles for these 3 samples determined by the best fits to the MEIS spectra are shown in Figure 8. Since the highest concentration part of the As

distribution nearest to the surface is removed by the wet clean, only the tail end of the original profile is retained in the sample. Thus, by overlaying the tail ends of the As depth profiles of samples AM1 and AM2 such that they coincide, which the Si profiles then also do, it becomes clear that the wet clean has removed the equivalent of 7 nm of the original top surface. Note that because of the removal of the top layer the originally

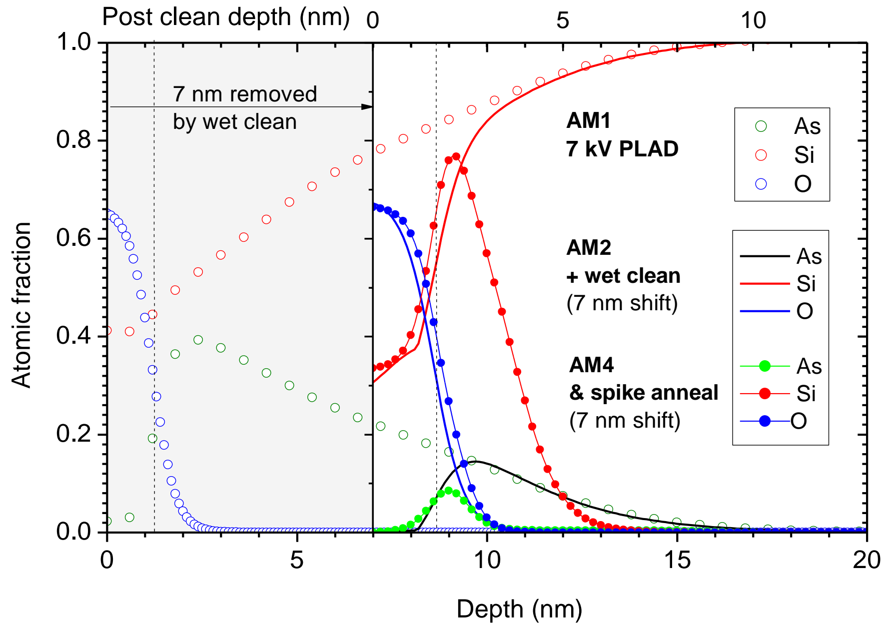

FIG. 8. Fractional depth profiles of As, Si and O of samples AM1, AM2 and AM4, showing the removal of the top 7 nm of the mixed Si/As layer by the wet clean including the loss of ~ 80% As and the solid phase epitaxial regrowth and As segregation under a 1.6 nm thick oxide after annealing. Process details are shown under the sample labels.

deeper located, remaining As peak is now closer to the surface and hence appears at the higher energy of 88 keV in the MEIS spectrum. It is clear from the figure that the SPM wet clean is effective in removing As from the mixed As/Si layer until the Si fraction exceeds 0.8 or concentration ~ 4 x 10^{22} cm^{-2} (see Fig. 1) at which point the As fraction has dropped to below 0.2 or concentration ~1 x 10^{22} cm^{-3}. Figure 8 also shows that the

As visible in sample AM2 is located underneath a thin oxide of ~ 1.6 nm, as indicated by the dotted marker line at half height of the O profile.

The depth profiles for the post spike anneal sample AM4 included in Figure 8, show the SPER induced redistribution of the visible As and the increased abruptness of the Si edge, already mentioned. Note that the Si profile for sample AM4 is not strictly a depth profile, since it is derived from a MEIS Si surface peak, recorded under aligned conditions. The thickness of the oxide layer has remained nearly unchanged. SPER causes As to become segregated and trapped under the oxide at a typical (inactive) dose of ~ 4 x 10^{14} cm^{-2}, somewhat less than 1 ML [12]. There is however more As retained in the sample to a depth of 10 nm that is not visible under double aligned conditions. This substitutional As dose can be determined from a comparison of the random and aligned As profiles, as is done in Section E.

Taking from Figure 8 that the top 7 nm was removed by this wet clean, it is of interest to estimate the numbers of Si atoms per cm^2 involved in the formation of the thick oxide as a result of the SPM wet etch and to compare this with the number of Si atoms per cm^2 contained in this top, 7 nm thick mixed As/Si layer. Using the information contained in this figure, while accounting for the Si densities of the mixed As/Si layer and the 1.2 nm oxide of sample AM1, adding the Si areal density of the 1.6 nm oxide of sample AM2 using the 10 % reduced oxide volume density as measured, this figure amounts to ~2.2 x 10^{16} Si cm^{-2}. Similarly, on the basis of the thickness for the oxide layer in in sample AM3.1 as determined by MEIS, a value of ~2.5 x 10^{16} Si cm^{-2} is calculated. These values suggest that all Si involved in the etched mixed As/Si layer is built into the oxide layer during the combined etch/oxidation and supports the need to invoke an extra

source of Si during the formation of the As/Si layer while undergoing PLAD, as is found to be the case during TRIDYN simulation of the overall PLAD process [4].

2. *Post anneal Random and Aligned spectra (non-oxydizing clean)*

The method for obtaining the angular conditions yielding random spectra off crystalline surfaces was described in section C. Figure 9 shows the random and aligned MEIS spectra for sample AM4 after spike annealing. The small O peak, clearly visible in the aligned spectrum, is due to a 1.6 nm thick oxide. The Si peak in the aligned spectrum does not reach the random level since it is the result of scattering off the reduced amount

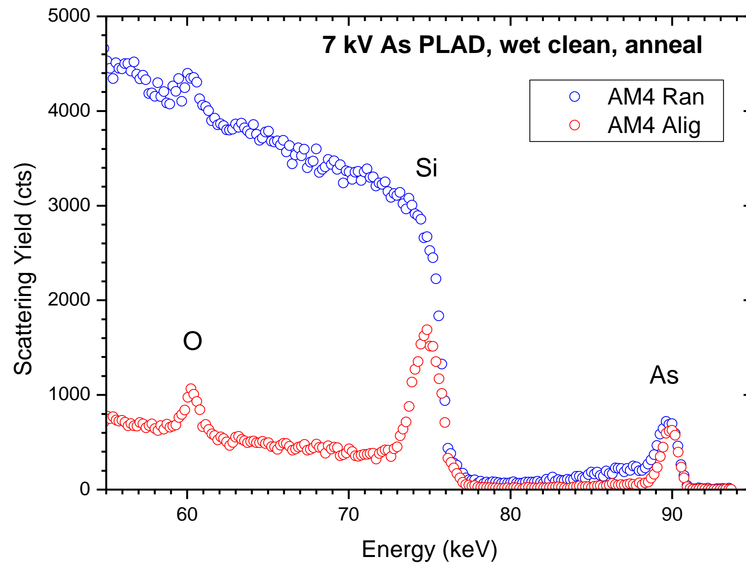

FIG. 9. MEIS energy spectra of AM4 (after 7kV PLAD, wet clean and spike anneal) in random and double aligned configurations.

of Si in the oxide including a narrow disordered underlying Si layer. The energy region above 80 keV comprising the As peaks, shows noticeable differences between the aligned and random spectra. These spectral regions were converted directly into As concentration

depth profiles for both the aligned and random conditions taking account of the change in illumination of the of the target by the ion beam [22]. The results are shown in Figure 10 and the difference profile, representing the substitutional As has been added. It is mentioned that there is a good correspondence between the profiles obtained from the IGOR model simulation (not shown) and the directly converted ones, however the former always show somewhat narrower profiles since the MEIS system resolution is deconvolved in the simulations.

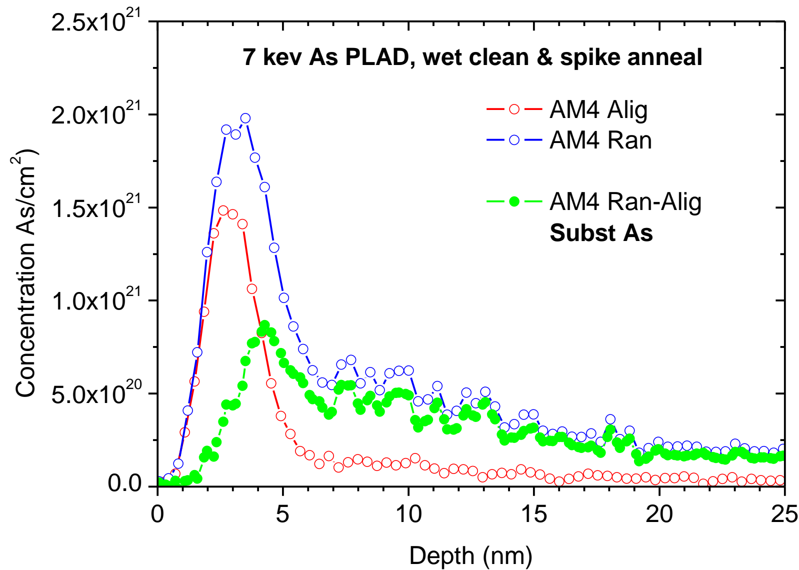

FIG. 10. As concentration depth profiles in sample AM4, converted from spectra taken in the random and aligned directions including the difference profile representing the substitutional As depth profile.

Integration of the areas of these three depth profiles gives the As doses retained for each case as given in Table III. Their difference represents the substitutional As dose of 8.0 x 10^{14} cm^{-2}. The area of the aligned profile of 5.5 x10^{14} cm^{-2} is predominantly made up of near-surface segregated As.

TABLE III. Retained As doses after PLAD at 7 kV bias, non-oxydizing wet clean and anneal, as measured in the random and aligned directions. The substitutional As doses, are given by their differences.

Sample	Integration over depth (nm)	As dose (cm^{-2}) Random	As dose (cm^{-2}) Aligned	As dose (cm^{-2}) Rand - Align (Subst. As)
AM4	0-25	1.35×10^{15}	5.5×10^{14}	8.0×10^{14}

Comparing this value for the retained dose with that obtained for the SPM clean sample AM3.2 of 1.35×10^{15} cm^{-2} As (having a thick surface oxide) as shown in Table II, it is seen that when using the SPM wet clean there is a significant, 70% increase in the retained substitutional As dose. Although the substitutional depth profiles for the two cases show somewhat different profile shapes, the ranges are similar, as expected. Figure 10 also shows that the doping concentration for this sample is typically around 5×10^{20} cm^{-3} over a depth of roughly between 3 and 13 nm.

D. Substitutional As dose and sheet resistance

In the above, the substitutional As doses determined were tacitly assumed to represent the active As dose in the sample. The aim in this section is to investigate the validity of this usual identification in the very near-surface region. Two Si samples, cut from the same wafer were given nominally the same 7 kV bias PLAD implant, SPM wet clean and a 1000°C spike anneal in N_2. However, they were measured to have sheet resistances of R_S ~300 Ω□ (sample AM3.9) and ~370 Ω□ (sample AM3.10), respectively. MEIS depth profile analysis was applied to determine their substitutional As profiles and doses, in order to investigate to extent to which substitutional dose values correlated with the different R_S values measured.

Energy spectra for the two samples AM3.9 and AM3.10 in both the aligned and random directions of incidence (not presented) showed no clear overall spectral differences, only subtle changes in the As peak regions. Therefore, only the derived As depth profiles in the random and aligned directions and their respective difference (Ran-Alig), or substitutional As profiles, are shown in Figure 11. The figure bears out in more detail the only small differences that can be seen in the As peaks regions of the energy spectra. Since for depths greater than 7 nm, the random depth profile for the lower sheet

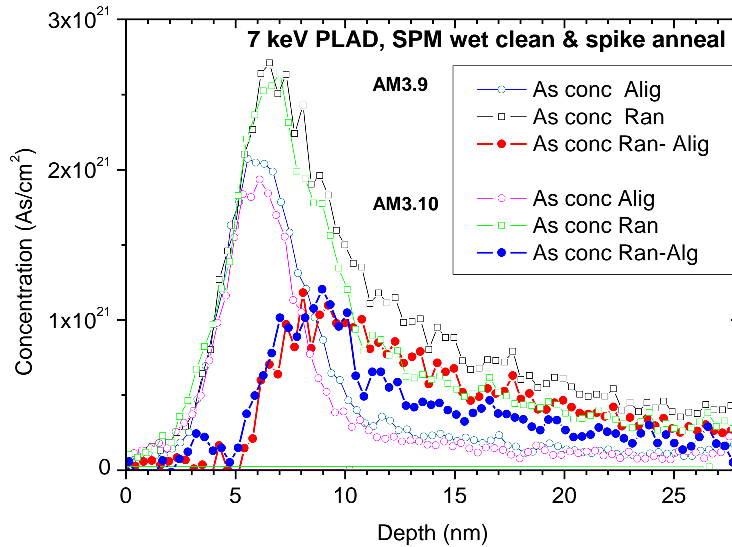

FIG.11. As concentration depth profiles of samples AM3.9 and 3.10, converted from spectra taken in the random and aligned directions, including their difference profiles. The measured ratio in substitutional doses corresponds closely with the inverse ratio of the sheet resistance measured for the two samples, indicating the validity of identifying the active with the substitutional dose for these nm thick, near surface implants.

resistance sample AM3.9 is clearly higher than that of the higher sheet resistance sample AM3.10, whilst the aligned spectra are not greatly different in height, it follows that the substitutional As dose N_s is greater for sample AM3.9 than that for sample AM3.10.

Quantification of the different As doses was achieved by integration of the depth profiles between 0 and 28 nm and for the substitutional As profiles, between 6 and 28 nm. The results are presented in Table IV.

Table IV shows that the low R_s sample AM.3.9 has an ~ 21% higher substitutional As dose, N_s, compared to the high R_s sample AM3.10, which is as expected. Considering the way R_s scales to N_s, for a uniformly doped, thin layer the sheet resistance can be shown to be inversely proportional to the charge carrier dose N_s [23]. The measured higher

TABLE IV. As doses retained after PLAD processing at 7 kV bias, SPM wet clean and anneal, measured in the random and aligned directions. The substitutional As doses, are given by their differences.

Sample	Integration over depth (nm)	As dose (cm^{-2}) Random	As dose (cm^{-2}) Aligned	As dose (cm^{-2}) Ran - Alig (Substit. As)
AM3.9	0 – 28 (6 – 28)	2.50×10^{15}	1.25×10^{15}	1.25×10^{15}
AM3.10	0 – 28 (6 – 28)	2.16×10^{15}	1.13×10^{15}	1.03×10^{15}

R_s value of ~370 Ω□, is 23 % higher than the lower one of ~300 Ω□. Assuming the validity of the mentioned relationship between R_s and the active dose N_s for the dopant profile in the near surface region of these samples, the correspondence between these two values is in fact excellent. It affirms that the higher R_s value is due to a lower active As dose measured and justifies the identification of the substitutional dose with the active dose in these very near surface conditions

SUMMARY AND CONCLUSIONS

Despite the growing application of PLAD in the production of microelectronic device, the details of the implanted and resulting active dopant profiles and their dependence on the parameters used in the PLAD process and subsequent processing are less well investigated and understood, primarily because of the limitations in depth resolution and sensitivity of available analytical techniques. Medium energy ion scattering (MEIS) depth profiling is perhaps uniquely capable of yielding high depth resolution, quantitative information on the structure and composition of nanolayers and hence provide details on the implant profile build-up inside the wafer surface during PLAD and subsequent processing, such as wet clean and spike anneal. MEIS analysis has been applied to investigate these device manufacturing stages. The main PLAD process considered was one where the wafer was pulse biased to 7 kV and exposed to ion doses of $1x10^{16}$ As cm^{-2}.

MEIS analysis showed that the above PLAD process using a 7 kV bias and a measured ion dose of $1x10^{16}$ As cm^{-2}, produced a near-triangular As depth profile with an As concentration near the surface of $2x10^{22}$ cm^{-3} (or ~40% As) which tails off over a depth of ~17 nm, in good agreement with XTEM EDS depth profiling measurements. The total retained As fluence is 1.6 $x10^{16}$ cm^{-2}. This layer is unstable in air and exposure causes SiO_2 formation and the loss of ~25% from the near-surface part of the As implant after 4 months.

A standard industry SPM wet clean containing an oxidising agent, removed As from the mixed As/Si layer and caused the concurrent formation of a ~14 nm thick oxide. A detailed comparison of aligned and random MEIS spectra of the implant after a 5s

1000°C spike anneal enabled the interstitial and substitutional As concentration depth profiles to be determined, including the retained doses. For the 7 kV PLAD process, they showed that following solid phase epitaxial regrowth of the disordered Si the substitutional As concentration was in excess of $1x10^{21}$ As cm^{-3} over a depth range of up to 10 nm, whilst a dose of ~5 x 10^{14} cm^{-2} of segregated, inactive As remained trapped under the surface oxide. Significantly, it is seen that the standard SPM clean leads to a more than 70% increase in the retained substitutional As dose compared to a non-oxidizing wet clean also investigated.

This non-oxidizing clean was found to remove a substantial part of As profile including the Si matrix. By matching the post clean MEIS As depth profile to the unetched tail of the original PLAD implant, it was found that the first 7 nm of the 17 nm intermixed As/Si layer was removed while the wet clean arrested at the point where the Si concentration had increased to 4 $x10^{22}$ cm^{-3}. Spike annealing again caused the segregation of As immediately under the oxide as well as a substitutional As dose of $8x10^{14}$ As cm^{-2}, having a concentration $5x10^{20}$ cm^{-3} to a depth of ~13 nm..

Substitutional doses in this near-surface configuration are shown to correlate well with sheet resistance measurements showing that their usual equating with the active As dose remains valid in the first 10 nm region considered. MEIS measurements as presented provide vital quantitative reference data for the TRIDYN based dynamic modelling approach that is being undertaken to understand the effects of the multiple interacting processes of deposition, (recoil) implantation and sputtering that occur in PLAD.

ACKNOWLEDGMENTS

J.E. would like to thank staff members at Varian Semiconductor Equipment Business Unit, Applied Materials in the Plasma Doping Group for preparing the samples and helpful discussions, especially Deven Raj who collected the first set of data that suggested this study, but also Cuiyang Wang, Harold Persing and Nicholas Chamberlain.

References

[1] Shu Qin, Y.J. Hu, and A. McTeer, in *2012 12th Int. Work. Junction Technol.* (IEEE, 2012), pp. 1–11.

[2] C. Wang, J. England, H. Gossmann, H. Persing, T. Miller, Q. Gao, S. Tang, and S. Salimian, in *2017 17th Int. Work. Junction Technol.* (IEEE, 2017), pp. 58–61.

[3] A. Renau, in *ECS Trans.* (The Electrochemical Society, 2011), pp. 173–184.

[4] J. England, W. Möller, J.A. van den Berg, A. Rossall, W.J. Min, and J. Kim, Nucl. Instruments Methods Phys. Res. Sect. B Beam Interact. with Mater. Atoms **409**, 60 (2017).

[5] S. Qin, Y.J. Hu, and A. McTeer, in *2010 Int. Work. Junction Technol. Ext. Abstr.* (IEEE, 2010), pp. 1–6.

[6] E. Demenev, D. Giubertoni, J. van den Berg, M. Reading, and M. Bersani, Nucl. Instruments Methods Phys. Res. Sect. B Beam Interact. with Mater. Atoms **273**, 192 (2012).

[7] F. Meirer, D. Giubertoni, E. Demenev, L. Vanzetti, S. Gennaro, M. Fedrizzi, G. Pepponi, A. Mehta, P. Pianetta, G. Steinhauser, V. Vishwanath, M. Foad, and M. Bersani, Appl. Phys. Lett. **101**, 232107 (2012).

[8] F. Meirer, E. Demenev, D. Giubertoni, L. Vanzetti, S. Gennaro, M. Fedrizzi, G. Pepponi, G.

Steinhauser, V. Vishwanath, M. Foad, and M. Bersani, Phys. Status Solidi **11**, 28 (2014).

[9] C. Jeynes and C., Nucl. Instruments Methods Phys. Res. Sect. B Beam Interact. with Mater. Atoms **406**, 30 (2017).

[10] J.F. van der Veen, *Surface Science Reports | Vol 5, Issues 5–6, Pages 199-287 (December 1985) | ScienceDirect.Com* (1985).

[11] R. Tromp, in *Pract. Surf. Anal. Vol. 2. Ion Neutral Spectrosc. 2nd Ed.* (Wiley, 1990), pp. 577–613.

[12] J.A. Van den Berg, D.G. Armour, S. Zhang, S. Whelan, H. Ohno, T.-S. Wang, A.G. Cullis, E.H.J. Collart, R.D. Goldberg, P. Bailey, and T.C.Q. Noakes, J. Vac. Sci. Technol. B Microelectron. Nanom. Struct. **20**, 974 (2002).

[13] M. Werner, J.A. van den Berg, D.G. Armour, W. Vandervorst, E.H.J. Collart, R.D. Goldberg, P. Bailey, and T.C.Q. Noakes, Nucl. Instruments Methods Phys. Res. Sect. B Beam Interact. with Mater. Atoms **216**, 67 (2004).

[14] W.-K. Chu, J.W. Mayer, and M.-A. Nicolet, *Backscattering Spectrometry* (Academic Press, 1978).

[15] J.F. Ziegler, M.D. Ziegler, and J.P. Biersack, Nucl. Instruments Methods Phys. Res. Sect. B Beam Interact. with Mater. Atoms **268**, 1818 (2010).

[16] IGOR Pro 6, Wavemetrics (2015).

[17] M.A. Reading, J.A. van den Berg, P.C. Zalm, D.G. Armour, P. Bailey, T.C.Q. Noakes, A. Parisini, T. Conard, and S. De Gendt, J. Vac. Sci. Technol. B, Nanotechnol. Microelectron. Mater. Process. Meas. Phenom. **28**, C1C65 (2010).

[18] H.H. Andersen, F. Besenbacher, P. Loftager, and W. Möller, Phys. Rev. A **21**, 1891 (1980).

[19] Data provided by C A Evans Associates.

[20] S.M. Shubeita, R.C. Fadanelli, J.F. Dias, and P.L. Grande, Surf. Sci. **608**, 292 (2013).

[21] L.C. Feldman and J.W. Mayer, *Fundamentals of Surface and Thin Film Analysis* (North-Holland, 1986).

[22] M.A. Nastasi, J.W. Mayer, and J.K. (James K. Hirvonen, *Ion-Solid Interactions : Fundamentals and Applications* (Cambridge University Press, 1996).

[23] J.W. Mayer and S.S. Lau, *Electronic Materials Science: For Integrated Circuits in Si and GaAs* (Macmillan, 1990).